geosciences

MDPI

*Article*

# Eocene Gravity Flows in the Internal Prebetic (Betic Cordillera, SE Spain): A Vestige of an Ilerdian Lost Carbonate Platform in the South Iberian Margin

**Josep Tosquella [1], Manuel Martín-Martín [2,*], Crina Miclăuș [3], José Enrique Tent-Manclús [2], Francisco Serrano [4] and José Antonio Martín-Pérez [2]**

[1] Departamento de Ciencias de la Tierra, University of Huelva, Campus Universitario del Carmen, 21071 Huelva, Spain; josep@uhu.es
[2] Departamento de Ciencias de la Tierra y Medio Ambiente, University of Alicante, AP 99, 03080 Alicante, Spain; je.tent@ua.es (J.E.T.-M.); jamartinperez@yahoo.es (J.A.M.-P.)
[3] Departamentul de Geologie, Universitatea "Alexandru Ioan Cuza" din Iași, 20A, Carol I, 700505 Iași, Romania; miclaus@uaic.ro
[4] Departamento de Ecología y Geología, University of Málaga, 28071 Málaga, Spain; f.serrano@uma.es
* Correspondence: manuel.martin.m3@gmail.com

**Abstract:** In the Betic-Rif Cordilleras, recent works have evidenced the existence of well-developed Eocene (Ypresian-Bartonian) carbonate platforms rich in Larger Benthic Foraminifera (LBF). Contrarily to other sectors of the western Tethys, like the Pyrenean domain in the North Iberian Margin, where these platforms started in the early Ypresian (Ilerdian), in the Betic-Rif chains, the recorded Eocene platforms started in the late Ypresian (Cuisian) after a widespread gap of sedimentation including the Ilerdian time span. In this work, the Aspe-Terreros Prebetic section (External Betic Zone) is studied. An Eocene succession with gravity flow deposits consisting of terrigenous and bioclastic turbidites, as well as olistostromes with olistoliths, was detected. In one of these turbidites, we dated (with the inherent limitations when dating bioclasts contained by gravity flow deposits) the middle Ilerdian, on the basis of LBF, representing a vestige of a missing Illerdian carbonate platform. The microfacies of these turbidites and olistoliths rich in LBF have been described and documented in detail. The gap in the sedimentary record and absence of Ilerdian platforms in the Betic-Rif Cordillera have been related to the so-called Eo-Alpine tectonics (Cretaceous to Paleogene) and sea-level variations contemporarily with the establishment of shallow marine realms in the margins of the western Tethys.

**Keywords:** lost Ilerdian carbonate platforms; Prebetic; South Iberian Margin; Eo-Alpine tectonics; microfacies characterization



Academic Editor: José Manuel Castro

Received: 28 January 2025
Revised: 18 February 2025
Accepted: 20 February 2025
Published: 23 February 2025

**Citation:** Tosquella, J.; Martín-Martín, M.; Miclăuș, C.; Tent-Manclús, J.E.; Serrano, F.; Martín-Pérez, J.A. Eocene Gravity Flows in the Internal Prebetic (Betic Cordillera, SE Spain): A Vestige of an Ilerdian Lost Carbonate Platform in the South Iberian Margin. *Geosciences* **2025**, *15*, 81. https://doi.org/10.3390/geosciences15030081



## 1. Introduction

In the Betic Cordillera (and also in the Rif Chain), recent works [1–6] have evidenced the existence of well-developed Eocene carbonate platforms rich in Larger Benthic Foraminifera (LBF) and zooxanthellate corals (z-corals) belonging to the meridional belt of platforms of the western Tethys. These platforms are usually dated as late Ypresian (Cuisian) to Lutetian or even reaching the Bartonian in a few cases. In contrast to other sectors of the western Tethys, such as the Pyrenean domain along the North Iberian Margin (northern belt of platforms), where these platforms are recorded since the early Ypresian (Ilerdian), in the Betic-Rif chains, the Eocene platforms began to develop in the late Ypresian (Cuisian). Consequently, no lower Ypresian (Ilerdian) deposits are known in the shallow

water record where most of the corresponding time span is represented by an extended unconformity. The whole Eocene has been registered only in the deep marine successions [6–8]. In this work, the Aspe-Terreros Prebetic section (External Betic Zone) in the Alicante province (SE, Spain) is studied in detail. This section shows a slope to deep basin sedimentary succession with interbedded gravity flow deposits [6]. In its lower part, terrigenous and bioclastic turbidites and olistostrome deposits containing carbonate platform olistoliths were detected [6]. The entire succession, as well as the olistoliths, have been dated with planktonic foraminifera and LBF. The microfacies of the bioclastic turbidites and the olistoliths rich in LBF are described and documented in detail. As is presented below, the age obtained on the basis of LBF from turbidites indicates an unknown time interval both in the platform successions of the Betic Cordillera and of the Rif Chain. The key contribution of this work is the identification of an unknown time interval (middle Ilerdian) based on LBF collected from gravity flow deposits and its implications for the Eocene evolution of the westernmost Tethys domains. Also, this work fills critical gaps in understanding the sedimentary and paleogeographic evolution of the region.

## 2. Geological Framework

The Betic Cordillera (Figure 1A) is classically divided into Internal and External Zones, with the Maghrebian Flysch Basin Units in between [7]. This cordillera belongs to the westernmost Mediterranean Alpine Belts (Figure 1B). The External Zone, the study area of this work, is, in turn, divided into two domains: the shallow marine Prebetic, stratigraphically continuous with the northern foreland (Iberian Meseta), and the pelagic Subbetic (southward from the Prebetic). These units have the status of tectono-paleogeographic domains and correspond to the South Iberian Margin (Figure 1B). In turn, both domains are subdivided into several sub-domains. In the case of the Prebetic, it is divided from north to south, in the External Prebetic (shallower) and the Internal Prebetic (deeper). All the South Iberian Margin domains consist of Triassic to Cenozoic sedimentary rocks that were progressively structured during the Middle-Late Miocene, from south to north, as a nappe stack [8]. Several works have been performed in the last decades in the Cenozoic succession of the Prebetics [6,8–27], distinguishing two different sedimentation areas: one related to a shallow marine nummulitids-rich platform to the NW and a deeper one with mass flow deposits (turbidites, olistoliths and olistostromes) related to an active Paleogene tectonics [27,28]. The Paleogene stratigraphy of Prebetics was well defined by Guerrera et al. [28], who distinguished the shallow Eocene nummulitids-rich platforms in the anticlines (Miñano Fm) from deeper turbiditic sedimentation areas in the sinclines (Pinoso-Rasa Fm). Recently, in a broad study of the whole Paleocene–Eocene Prebetic succession from the whole Betic Cordillera, three informal stratigraphic formations were provisionally defined since their stratotypes were not properly established [6]: (1) the Paleocene to middle Lutetian lower marly-clayey fm; (2) the Cuisian to lower Bartonian intermediate limestone-calcarenite fm; and (3) the Lutetian to Priabonian upper marly-clayey fm. Diachronic boundaries were recognized within these stratigraphic units [6]. This informal stratigraphic nomenclature is used in this paper.

For this work, the Aspe-Terreros section studied in the above-mentioned paper [6] was revisited. This section belongs to the Internal Prebetic and is characterized by a marly deep-water succession rich in gravity flow deposits containing bioclasts reworked from Eocene carbonate platforms.

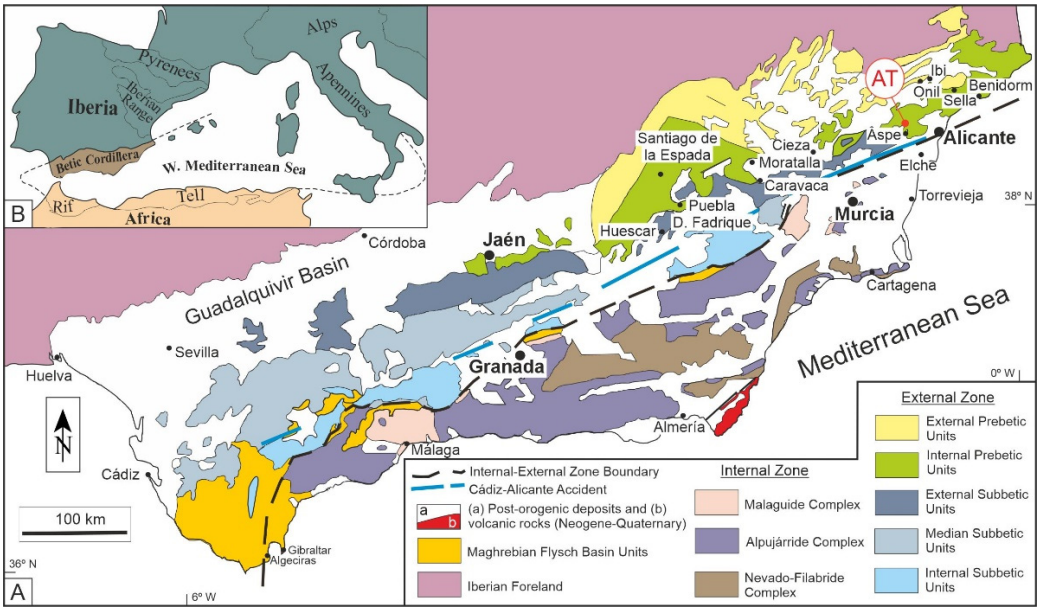


**Figure 1.** (**A**) Tectonic map of the Betic Cordillera (after [7]) showing the locations of the Aspe-Terreros section; (**B**) Alpine Chain map of the western-central Mediterranean area (modified from [5]).

## 3. Materials and Methods

The methods used in this study are:

(1) Field analyses included the logging and sampling (all samples were taken following standard procedures after removing the surficial cover) for microfacies analysis and for biostratigraphic studies (18 samples) of the Aspe-Terreros stratigraphic section (Table 1). Well-preserved rock samples were collected from the section, covering all the identified field lithofacies and increasing the sampling resolution where significant changes in sedimentary facies or palaeontological content occurred. For the construction of a geological map, an aerial photo was performed with our own drone (DJI air 2s) using the software dronelink. In an area of 0.300 km$^2$, 263 photos were taken.

(2) Laboratory analyses concerned microfacies, biostratigraphy, and bio-chronostratigraphy based on planktonic foraminifera, calcareous nannoplankton, and LBF. For the Eocene biostratigraphy, the following zonations were used: (1) planktonic foraminifera [29–31]; (2) LBF, the Shallow Benthic Zones (SBZ) [32]; and (3) calcareous nannoplankton [33]. The formal names of the taxa cited throughout the text are compiled in a taxonomic appendix added in Supplementary Materials. Analysis of microfacies was carried out by the study of standard thin sections (2.0 × 3.0 cm), following the methodology of Flügel [34], where the percentages of fossil abundance were evaluated by point counting on the thin sections. The identification of larger foraminifera was performed following Loeblich and Tappan [35], where the genus *Assilina* includes both *Assilina* s.s. and 'operculiniform *Assilina*', as defined by Tosquella and Serra-Kiel [36]. Systematics of nummulitids is mainly based on Hottinger [37] and Schaub's [38] works. Paleobathymetric reconstructions of the LBF are mainly based on Hottiger [39], Baceta and Mateu-Vicens [40], and Mariani et al. [41]. Processed and illustrated studied samples, with their sampling numbers, are stored and available for future research in the Ecology and Geology Department of the University of Málaga (planktonic foraminifera) and in the Earth Sciences Department of the University of Huelva (LBF).

(3) Geological modeling during which the data obtained were processed to elaborate our interpretations and conclusions.

**Table 1.** Collected samples, field facies, and studied fossil groups.

| Samples | EP80a, EP95 and EP96 | EP80b, EP84, EP86 and EP93 | EP81–83 EP85, EP87–92, EP94, EP97 |
|---|---|---|---|
| Field facies | Bioclastic turbidites | Bioclastic turbidites | Mudstones |
| Studied fossil groups | LBF in loose samples | LBF in thin section | planktonic foraminifera and calcareous nannoplankton |

## 4. Results

### 4.1. Lithostratigraphy of the Aspe-Terreros Section

The sedimentary succession in Aspe-Terreros is discontinuously exposed around 150 m. It consists mainly of fine deposits belonging to the lower and upper marly-clayey fms [6] deposited onto a regional unconformity separating the Upper Cretaceous Capas Blancas Fm (Table 2) from the overlying Paleogene succession [27,28]. In the measured section, we could distinguish three different intervals belonging to the Eocene (Figure 2).

**Table 2.** Stratigraphic framework of the Aspe-Terreros section: formation names, intervals, and biostratigraphic ages.

| Stratigraphic Formation | Intervals | Age of the Deep-Water Sedimentation | Age of the Bioclasts |
|---|---|---|---|
| upper marly-clayey fm | Third interval | late Lutetian to Bartonian (E10–13 zone) | Cuisian (SBZ11) |
| lower marly-clayey fm | Second interval | early-middle Lutetian (E8-E9 zones) | |
| | First interval | Paleocene-early Lutetian (from the literature) | Ilerdian (SBZ8) |
| | Not studied | | |
| Capas Blancas Fm | Not studied | Senonian (from the literature) | |

The first interval (12 m exposed) is characterized by thick units of sandstones and rudstones occurring on a poorly exposed greenish-grey mudstone background (Figure 2B,C). The sandstone unit (>3 m thick) is made of several dm-thick beds with sharp lower bounding surfaces, either unstructured (with mudstone intraclasts) or with different internal structures, such as tabular sets (cm-thick) of crossed laminae, parallel laminae, or convolute lamination with overturned sharp anticlines and rounded synclines. Between the sandstone beds, there were probably thin mudstone interlayers that were not preserved. The rudstone unit (ca 3 m thick) is normally graded from bioclastic rudstone to bioclastic calcarenites. Its lower bounding surface has load casts. A rough bedding can be distinguished. The bioclasts are mostly nummulitids, the largest of them being imbricated. A sample (EP80a) was taken from the looser LBF forms at the base of a turbidite for biostratigraphic analysis, and one (EP80b) from the better-cemented portion for microfacies analysis of the same bed (Figure 3).

The second interval (ca 30 m thick) consists of soft light grey marls with disrupted interlayers of competent dm-thick marls/calcarenites (Figures 2B,C and 3B–E). Olistoliths of different sizes (from several decimeters to several meters in diameter) occur in the entire interval. Some of the competent marl beds are dismembered or contorted. Where recognizable, the bedding of this interval appears different from the first interval and also from the third interval. The contact between the first and second interval is sharp, and

the olistoliths occur from 1 m upward. Both soft and competent beds and the biggest olistolith were sampled (EP 81, 82, and 85 from fine material, EP84 from the olistolith). The competent beds are mostly fine-grained (marls), but some coarser ones show a rough lamination and can contain nummulitids and big clasts of whitish marls.

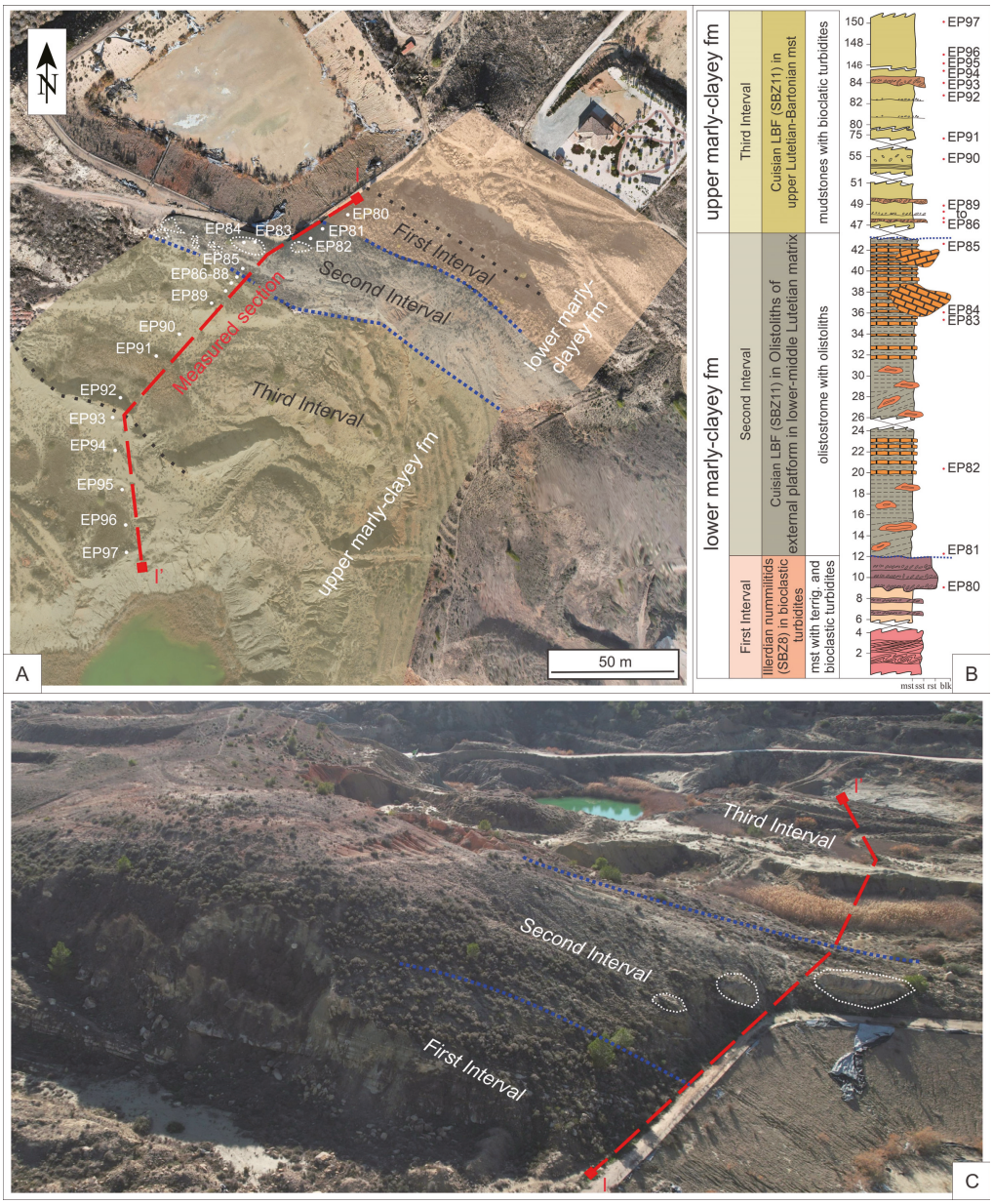


**Figure 2.** (**A**) Geological sketch map of the Aspe-Terreros area superimposed onto the aerial picture obtained by drone (the photo sets obtained during the drone flights were processed with WebODM software, obtaining 263 aligned pictures used to build a 3D model for an area of about 0.3145 km$^2$, 1,177,191 tie points, a dense point cloud of 24,805,637 points, and an average Ground Sampling Distance of 2.2 cm). The orthophotography obtained has a size of 15,009 × 14,425 pixels, showing the three main intervals (with locations of the measured section and the collected samples). (**B**) Stratigraphic column of the Aspe-Terreros area, showing the three main intervals, sedimentologic characteristics, and sample locations. (**C**) Aerial picture of the Aspe-Terreros studied section obtained by drone. In (**A**–**C**), dotted blue lines contour the second interval (olistostrome), while dotted white lines in the second interval contour the olistoliths. Legend for 2B: mst—mudstone; sst—sandstone; rst—rudstone; blk—blocks (olistoliths).

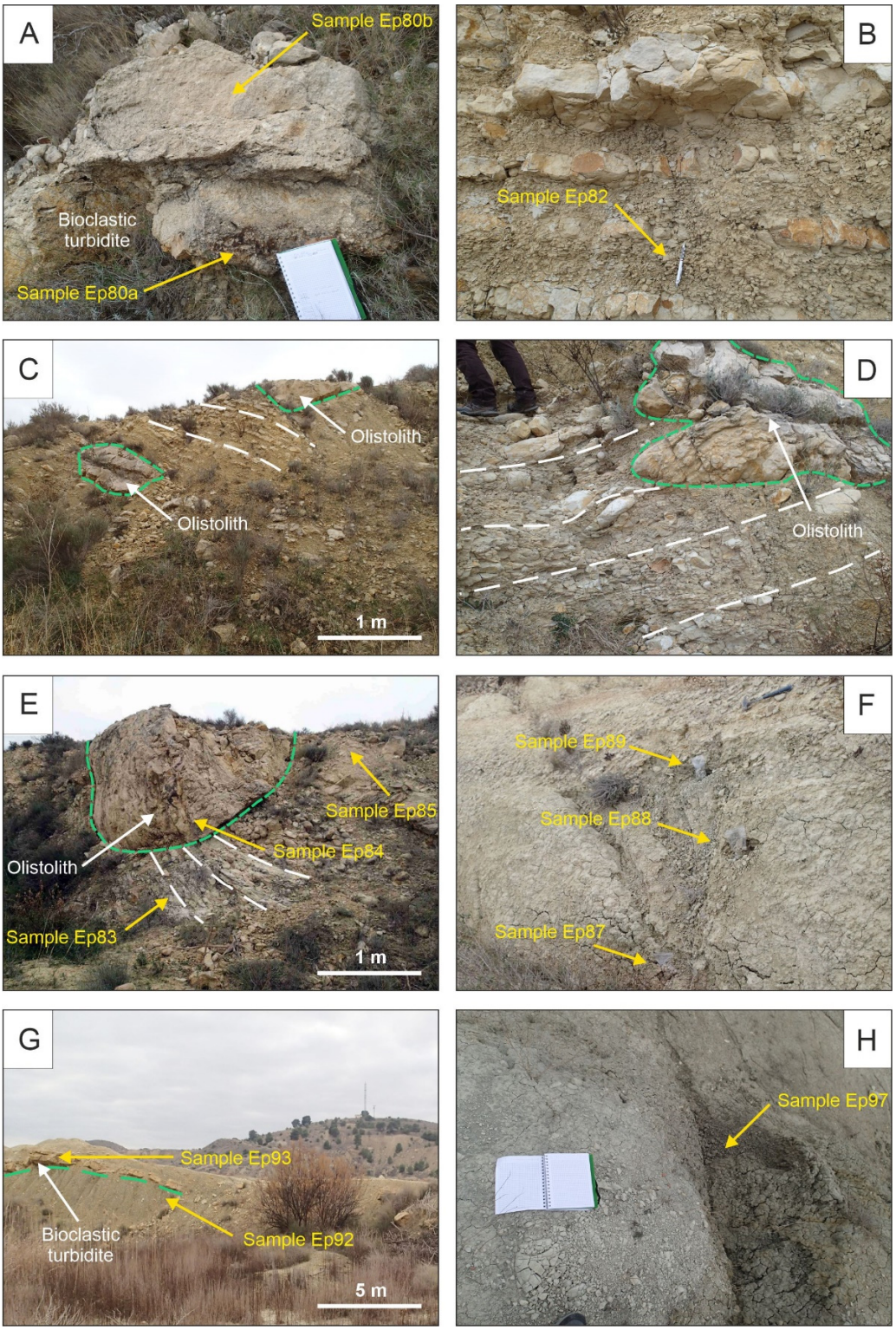


**Figure 3.** Field photos of the Aspe-Terreros section (**A**–**H** from bottom to top) with the location of the main samples (all samples were taken following standard procedures after removing the surficial cover). (**A**) Bioclastic turbidite in the first interval of the section (samples EP80a and EP80b); (**B**) preserved stratification of the olistostrome in the second interval of the section (sample EP82); (**C**,**D**) olistoliths in the second interval of the section; (**E**) large olistoliths in the second interval of the section (samples EP83 to EP85); (**F**) mudstones from the third interval of the section (samples EP87 to EP89); (**G**) mudstones with bioclastic turbidite in the third interval of the section (samples EP92 and EP93); (**H**) dark greyish to greenish marls and clays in the top of the section (sample EP97).

The third interval (ca 100 m) consists mainly of greenish-grey mudstone with some interlayers of bioclastic sandstones and rudstones with variable thickness (a few cms to 60 cms), which can be followed tens of meters along the outcrop (Figures 2B,C and 3F–H). From the coarse-grained bioclastic interlayers, samples EP86 (thin interlayer) and EP93 (thickest interlayer) were taken for microfacies analysis. The bioclastic beds have a sharp erosive lower bounding surfaces, and the thickest bed also has loadcasts. Some interlayers of light reddish or green laminated mudstones can be observed. The mudstone embedding the bioclastic interlayers were sampled (EP87–89, EP92, and EP97 for planktonics; EP90, EP94–96 are collections of nummulites and alveolines).

### 4.2. Age of the Sedimentary Succession

Two kinds of ages are obtained in the section: (1) the age of the deep-water deposits (authochthonous pelagic and hemipelagic mudstones mostly from the third interval) and the matrix of the olistostrome dated with planktonic foraminifera (Figure 4) and calcareous nannoplankton; (2) the age of the resedimented material making part of the olistoliths and the bioclastic turbidites dated with LBF (Figure 5) with the expected limitations peculiar to dating bioclasts contained in gravity flow deposits. The age of the entire studied stratigraphic section is early–middle Lutetian to Bartonian. The lowermost dated levels of the olistostrome matrix (supposedly of authochthonous deep-water sedimentation) in the section correspond with the base of the second interval of the section. In these samples, the E8–E9 zones (early–middle Lutetian) have been dated by the presence of *Acarinina bullbrooki*, *A. cuneicamerata*, *Morozovella aragonensis*, and *Morozovelloides crassatus*. Also, calcareous nannoplankton has been found in these levels (*Reticulonenestra umbilica*, *Ericsonia formosa*, and *Chiasmolithus gigas*), dating the Lutetian without more precision. The top part of the olistostrome yielded a poor assemblage with *Igorina broedermanni*, *A. bullbrooki*, *A. praetopilensis*, *T. frontosa*, and *T. possagnoensis*, indicating the E9 zone (middle Lutetian). In the third interval of the section, the E9 zone (middle Lutetian) is dated by the presence of *Acarinina bullbrooki*, *A. praetopilensis* (some specimens close to *Acarinina topilensis*), *M. aragonensis*, *M. crassatus*, *Morozovelloides coronatus*, and *Globigerinatheka subconglobata*, together with *Subbotina eocaena* and *Subbotina corpulenta*. Towards the upper part of the section, the E10 zone (late Lutetian) is confirmed by the presence of abundant forms of *Acarinina* and *Morozovelloides*, but the absence of *Morozovella* ones as that of the *M. aragonensis* group. The uppermost part of the section yielded *Subbotina gortani*, *Turborotalia pomeroli*, *Turborotalia cerroazulensis*, and *Pseudohastigerina micra* together with the persistence of Morozovelloides. This association characterizes the E13 zone of the Bartonian. The upper part of the section is also dated with calcareous nannoplankton as Lutetian-Bartonian transition (NP16–17 zones) by the presence of *Ericsonia formosa*, *Reticulofenestra umbilica*, and *Chiasmolithus grandis*.

Both the age of olistoliths in the olistostrome and the bioclastic turbidites of the third interval are Cuisian. A different age was obtained for the bioclastic turbidite in the first interval, which provided an Ilerdian assemblage. In detail, sample EP80a was dated SBZ8 (late middle Ilerdian) by the presence of *Nummulites spirectypus*, *N. exilis*, *N. atacicus*, *N. globulus laxiformis*, *Assilina canalifera*, and *As. ammonea ammonea* (Figure 5). From sample EP80b to EP96, several SBZ11 (middle Cuisian) LBF associations were found: EP80b (*N.* cf. *cantabricus*, *N.* cf. *praelaevigatus*, *N. aff. manfredi*, *Assilina placentula*, *As. marinellii*, and *Alveolina cosigena cosigena*), EP84 (*Ornatorotalia? granum*, *Granorotalia sublobata*, *Rotalia aff. trochidiformis*, and *Gyroidinella levis*), EP86 (*Ornatorotalia granum*), EP93 (*N.* cf. *cantabricus*, *As. karreri*, *As. aff. parva*, *As. marinellii*, *Cuvillerina* cf. *vallensis*, and *Ornatorotalia granum*), EP95 (*Nummulites pavloveci*, *N. pustulosus*, *N. burdigalensis pergranulatus*, *N. irregularis*, *N. aff. formosus*, *N.* cf. *distans*, *Assilina placentula*, *As. laxispira*, *As. escheri*, and *As. marinellii*), and

EP96 (*Nummulites pavloveci*, *N. pustulosus*, *N. burdigalensis pergranulatus*, *N. irregularis*, *N. aff. formosus*, *N. distans*, *Assilina placentula*, *As. escheri*, and *As. marinellii*).

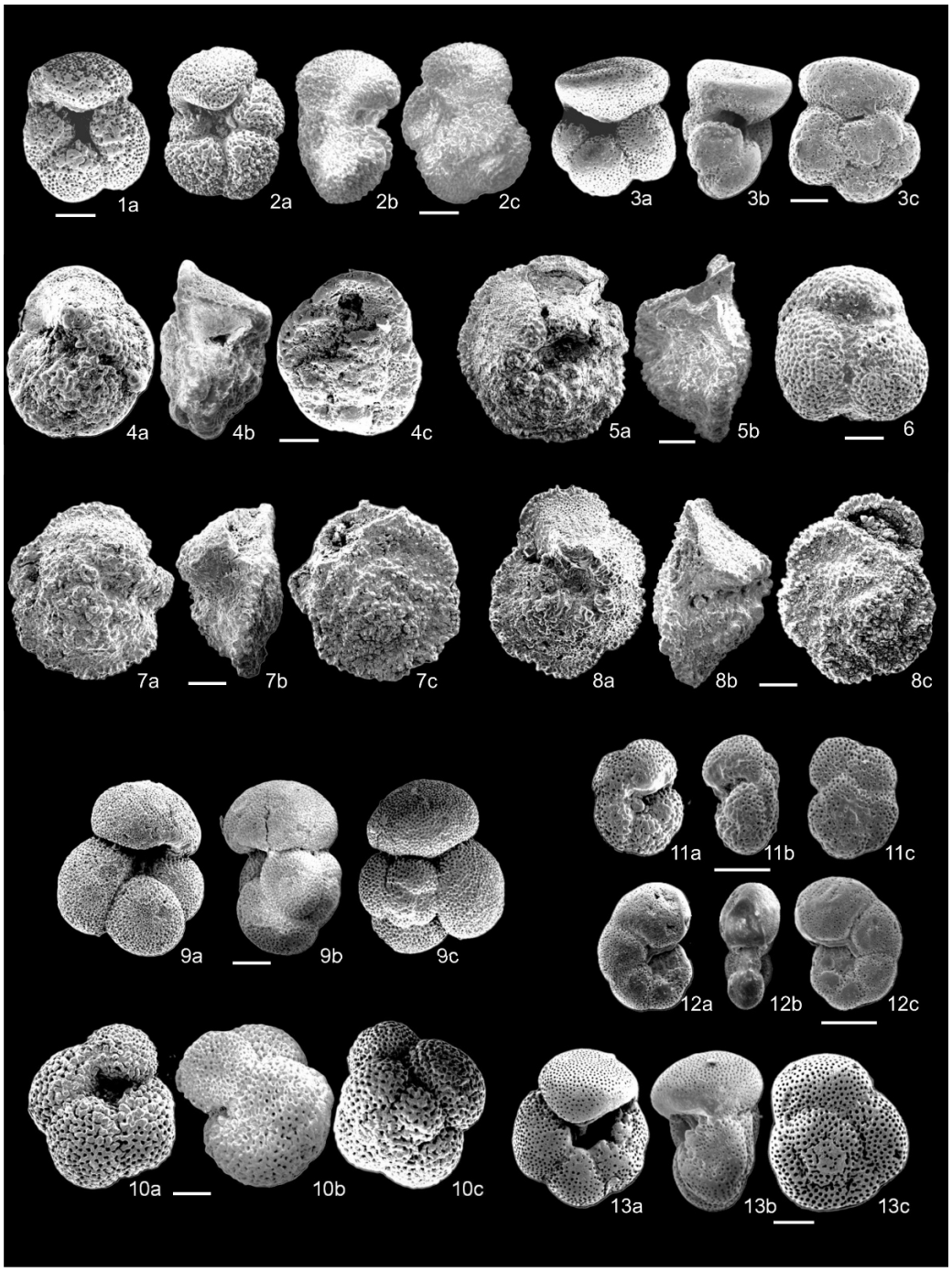


**Figure 4.** Significant planktonic foraminifera from the Aspe-Terreros section. Scale bar = 100 μm. **1a**: *Acarinina bullbrooki*, EP89. **2a–c**: *Acarinina cuneicamerata*, EP88. **3a–c**: *Acarinina praetopilensis*, EP87. **4a–c**: *Morozovella aragonensis*, EP88. **5a–b**: *Morozovella crater*, EP88. **6**: *Globigerinatheka subconglobata*, EP88. **7a–c**: *Morozovelloides crassatus*, EP87. **8a–c**: *Morozovelloides coronatus*, EP97. **9a–c**: *Subbotina eocaena*, EP97. **10a–c**: *Subbotina gortanii*, EP97. **11a–c**: *Igorina broedermanni*, EP88. **12a–c**: *Pseudohastigerina micra*, EP97. **13a–c**: *Turborotalia pomeroli*, EP97. Illustrated studied samples are stored and available, with their sampling numbers, for future research in the Ecology and Geology Department of the University of Málaga.

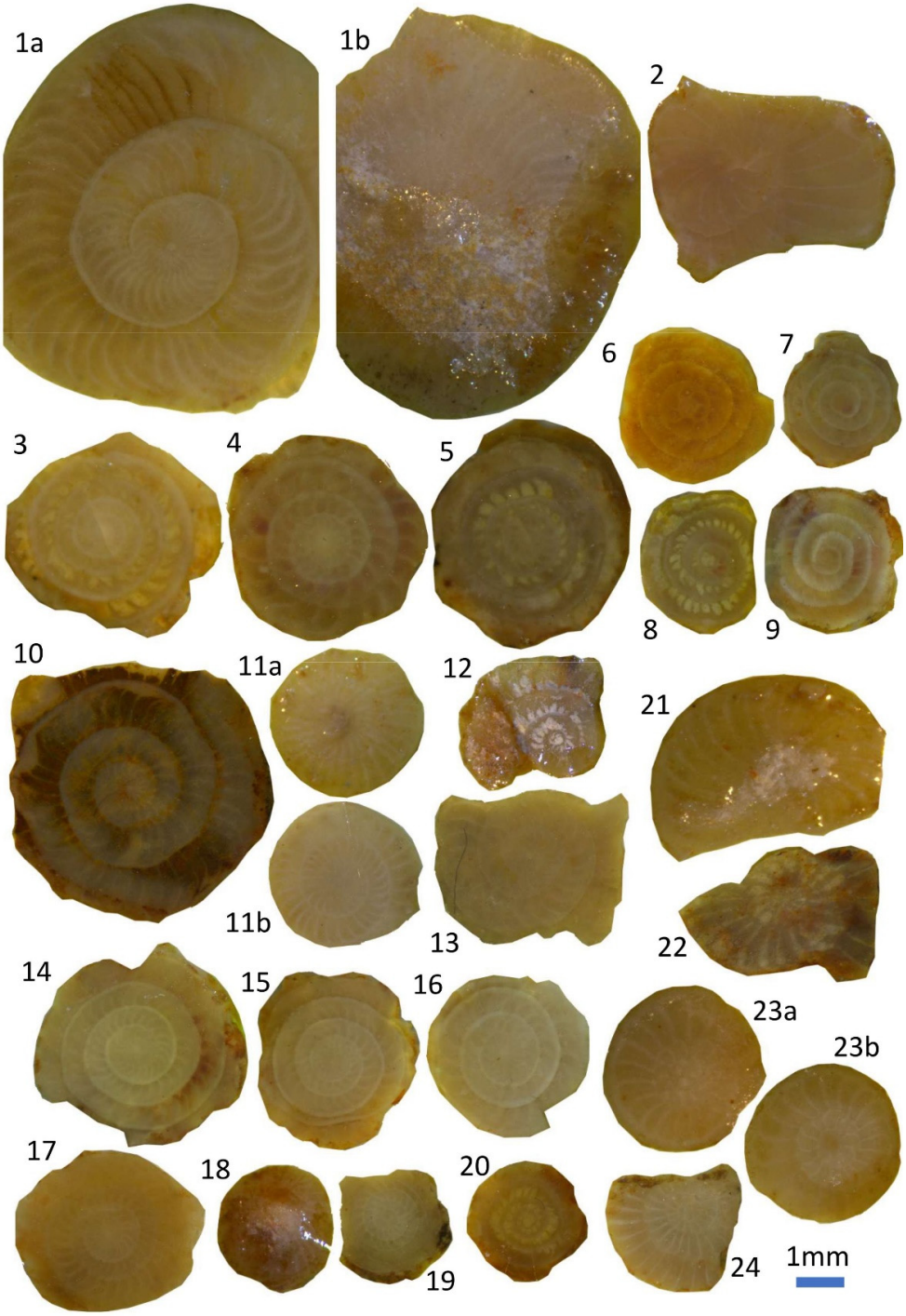


**Figure 5.** Main LBF biomarker species of the late middle Ilerdian (SBZ8) from a bioclastic turbidite of the first interval of the Aspe-Terreros section (EP80a). **1–2**, *Nummulites spirectypus*: **1a**, BF internal view; **1b**, BF, external view; **2**, AF, internal view. **3–9**, *Nummulites atacicus*. **3–5**, BF, internal views; **6–9**, AF, internal views. **10–13**, *Nummulites exilis*: **10**, **11b**, BF internal views; **11a**, BF external view; **12–13**, AF internal views. **14–20**, *Nummulites globulus laxiformis*: **14–17**, BF internal views; **18**, AF external view; **19–20**, AA, internal views. **21–22**, *Assilina canalifera*: AF external views. **23–24**, *Assilina ammonea ammonea*: **23a**, AF external view; **23b–24**, AF internal views. Scale: 1 mm. AF: A-forms (gamonts); BF: B-forms (agamonts or schizonts). Illustrated studied samples, with their sampling numbers, are stored and available for future research in the Earth Sciences Department of the University of Huelva.

### *4.3. Microfacies Description*

Two main microfacies (Mf1 and Mf2) indicating mid (e.g., sample EP80b) and outer ramp/upper slope (e.g., sample EP84) sources (Ilerdian to Cuisian in age) for the bioclastic

turbidites and olistoliths have been recognized in the first and second intervals of the studied section (Figure 6).

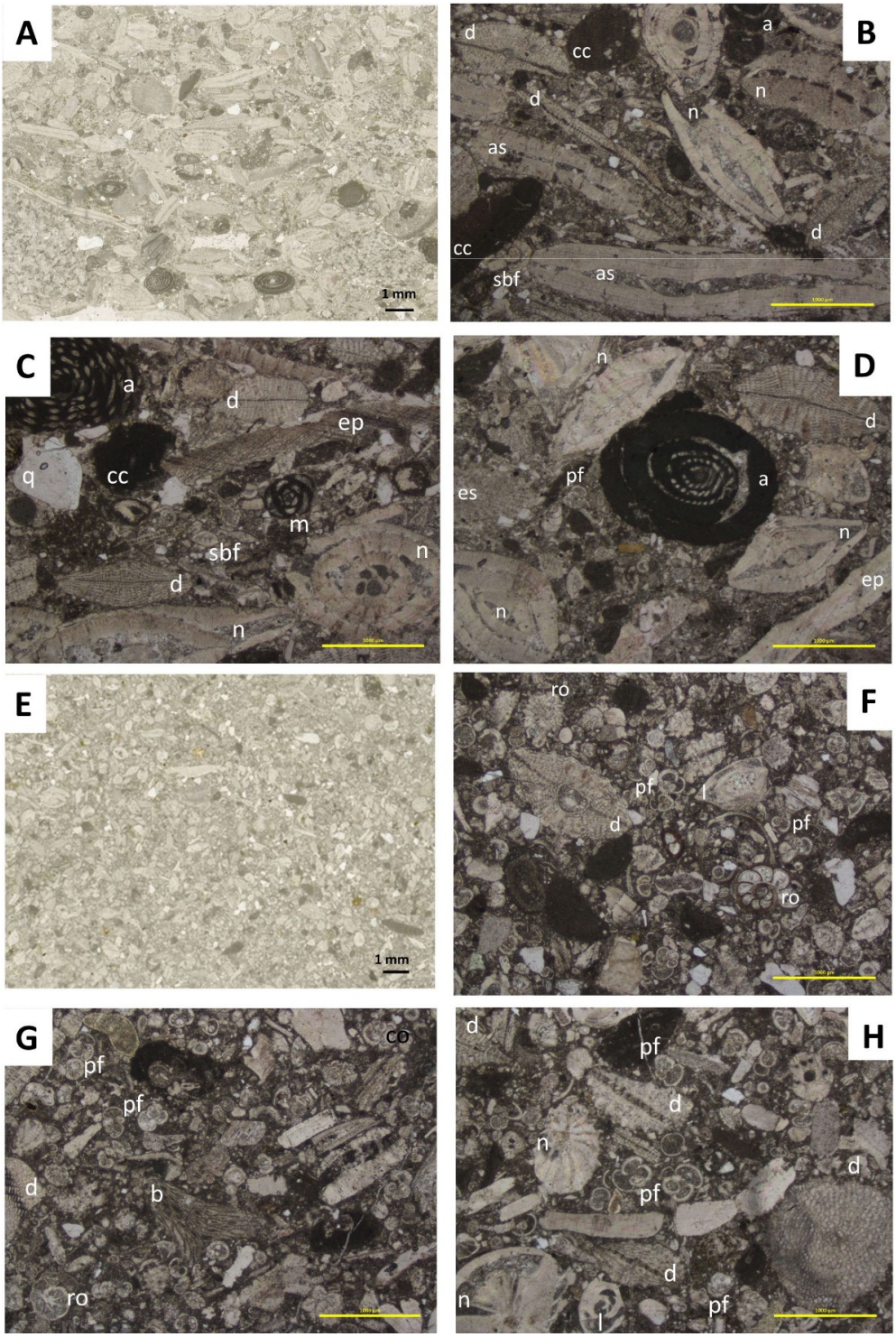


**Figure 6.** Thin section photomicrographs of the microfacies recognized in the bioclastic turbidite and olistolith of the Aspe-Terreros section. (**A**–**D**) Microfacies 1 (sample EP80b). (**E**–**H**) Microfacies 2 (sample EP84). Scale: 1.0 mm. Key: a, *Alveolina*; as, *Assilina*; b, bryozoan; cc, crustose coralline; d, *Discocyclina*; ep, echinoid plate; es, echinoid spine; l, *Lenticulina*; m, miliolid; n, *Nummulites*; pf, planktonic foraminifera; q, quartz grain; ro, rotaliid; sbf, small benthic foraminifera.

Microfacies 1 (Mf1) is made of packstone-grainstone of LBF reoriented tests (EP80b). These microfacies have been observed in the lowermost part of the Aspe-Terreros section in the base of the bioclastic turbidite. It is a moderate to well-sorted facies and presents a compact texture made up of abundant planar tests of mainly hyaline LBF; it also includes some taxa with porcelaneous walls. The LBF association is made up of *Discocyclina* (25–30%), flat *Nummulites* (15–25%), *Assilina* and operculiniform *Assilina* (10–15%), *Alveolina* (5–10%), and *Orbitolites* (5%). Other elements such as rotaliids (5–10%), remains of echinoids (5–10%), and crustose coralline algae (5%) can be common. Occasionally, scarce annelids (*Ditrupa*, 2–3%), planktonic foraminifera (2–3%), miliolids (2–3%), textulariids (2–3%), and other unspecified small benthic foraminifera (1–2%) can be recognized. Frequently, small angular quartz grains are also observed (3–5%). The good sorting of tests by size and common orientation of the largest bioclasts is consistent with reworking by unidirectional currents in deeper sedimentary environments (turbidite currents). The conspicuous presence of quartz grains indicates energetic events that affected the shallow water platform, while the low presence of planktonic foraminifera suggests that the source of bioclasts was a mid-ramp sedimentary environment. In general, hyaline tests with a flattened morphology (flat *Nummulites*, *Assilina*, operculiniform *Assilina*, and flattened *Discocyclina*) predominate, although a prevalence of porcellaneous elements is also observed locally. Considering the flattened-test LBFs thrive in deeper conditions [39,42–47], their predominance would indicate that reworked material was supplied from the deeper areas of the mid-ramp [2,3,39,41].

Microfacies 2 (Mf2) is made of planktonic foraminiferal-rich bioclastic packstone (EP 84). Thise microfacies was described based on a sample taken from the largest olistolith in the olistostrome. It is a well-sorted facies constituted by fine-grained sediment mainly composed of planktonic (15%) and small benthic foraminifera (15%), rotaliids (10–15%), echinoid plates and spines (5%), fragments of crustose coralline algae (5%), vinculariform bryozoans (5%), and hyaline LBF tests mainly of *Discocyclina* (5–10%), *Assilina* and operculiniform *Assilina* (5%), *Amphistegina* (5%), *Nummulites* (5%), some agglutinated ones as textulariids (2–5%), and porcelaneous as *Alveolina* (2–3%). Small angular quartz grains can also be common (5–10%). The fabric is well sorted, without a muddy matrix, and dominated by planktonic foraminifera, displaying a common orientation. The fragments of hyaline LBF tests (mainly of *Discocyclina* and *Amphistegina*) occur in the reworked levels. These flat LBF tests are usually developed in low luminosity habitats in the outer ramp or upper slope environments [2,3,39,41].

## 5. Discussion

The above-presented results allow us to discuss the age and the corresponding sedimentary realms of the defined intervals in the studied section in the following lines, as well as obtain important deductions about the source area. All our results are integrated with data from the literature in the region. The implications for the Eocene evolution of the westernmost Tethys domains are also presented.

The above-mentioned features of sandstone beds (sharp lower bounding surfaces; the unstructured appearance; and/or the different internal structures, such as crossed laminae, parallel laminae or convolute lamination with overturned sharp anticlines, and rounded synclines) from the first interval of the section indicate sedimentation by high- to low-density turbidity currents. Turbidity current is also the process of bioclastic unit sedimentation, but the transported and sedimented material consisted mainly of nummulitids. The thickness of sandstones and bioclastic rudstones, as well as the amalgamated character of the sandstone units, suggest a proximal sedimentation area in the turbiditic system.

The second interval contains dismembered beds and olistoliths. Moreover, this stratigraphic unit has a ”discordant” position in relation to both the first and third intervals. All

these features indicate that the entire unit is a big olistostrome with olistoliths sedimented by gravity slumping of not entirely consolidated deposits of the outer ramp/upper slope.

The third interval shows bioclastic turbidites sedimented on a muddy slope. The small thickness of most turbidite beds suggests a distal sedimentation area in the turbidite system. The entire section displays adeeepening upward trend.

In the entire section, LBFs in the bioclastic turbidites and olistoliths indicate, with the expected limitations when dating bioclasts contained by gravity flow deposits, resedimented material with ages ranging between SBZ8 and SBZ11 (late middle Ilerdian to middle Cuisian. Sample EP80a from the bioclastic turbidite of the first interval provided a late middle Ilerdian age. The Ilerdian is an interval usually missing in the Betic Cordillera, in particular in carbonate platform deposits [1–6]. There is a paper on the Internal Rif that describes the presence of Ilerdian resedimented material at a Cuisian platform level [48]. Recently, the widespread absence of Ilerdian platforms in these domains has been attributed to early Paleogene tectonics and/or a sea-level fall [1–6,27,28], causing the subaerial exposure of platforms, followed by erosion and unconformity development before the Cuisian transgression and the resumption of the sedimentation. Therefore, the sampled resedimented material may be one of the few known vestiges of a destroyed older (Ilerdian) carbonate platform. This a common situation in short-lived carbonate factories that may be uplifted and eroded, with all their in situ traces being removed [49]. However, their presence can be recognized on the basis of the resedimented materials within the deep-water deposits, offering the possibility to reconstruct the platform even if nothing remained in situ.

All the mentioned data and results, integrated with data from the literature in the region [6,25–28], allowed us to propose a scenario (Figure 7) for the way the Aspe-Terreros sedimentary succession was developed. The background sedimentation of the area is recognized in the first and third intervals, which both indicate a muddy slope (where pelagic-hemipelagic deposits are characteristic) sporadically crossed by turbidity currents. The turbidity currents were supplied by different sources: one terrigenous (e.g., sandstones), recognized in the lowermost part of the section (first interval), and the other bioclastic. The terrigenous source (derived from the Iberian Meseta) was active in early Ypresian—early Lutetian. Similar turbiditic sandstones, likely from the same source area, have been described in the western Murcia region, in the Pinoso-Rasa Formation [28], and, recently, as part of the lower marly-clayey fm in the Alicante area [6]. The novelty here is the source that supplied the bioclasts resedimented in the bioclastic turbidite. They were proved to be derived from an Ilerdian platform rich in LBF, which no longer exists in any studied area of the Betic-Rif Cordilleras. As mentioned above, the Ilerdian is represented by an unconformity covering the Paleocene–Eocene boundary time span in the Betic-Rif platform domains, but the fossil assemblage in the sampled turbidite bed (EP80a) shows that an Ilerdian shallow water platform existed. As the microfacies Mf1 indicates, the material was supplied from the mid-ramp. At the same time, the olistostrome "matrix" was dated based on planktonics as lower-middle Lutetian (EP81–85), but it contains olistoliths of older age. Their fossil content and microfacies indicate a Cuisian outer ramp/upper slope as the source area. This Cuisian platform must have been different (or formed later) from the Ilerdian one, as is proved by the biostratigraphic age and the microfacies features of the supplied olistoliths. The olistostrome could be the result of upper slope slumping likely caused by source platform uplifting contemporary with subsidence in the sedimentation area of the Aspe-Terreros section. In turn, the uplifting and subsidence may be consequences of faulting and folding related to the Paleogene tectonics (Eo-Alpine phase [50]) together with sea-level changes. The argument to support this proposal is that after the sedimentation of the olistostrome, the muddy slope was restored while the basin deepness increased.

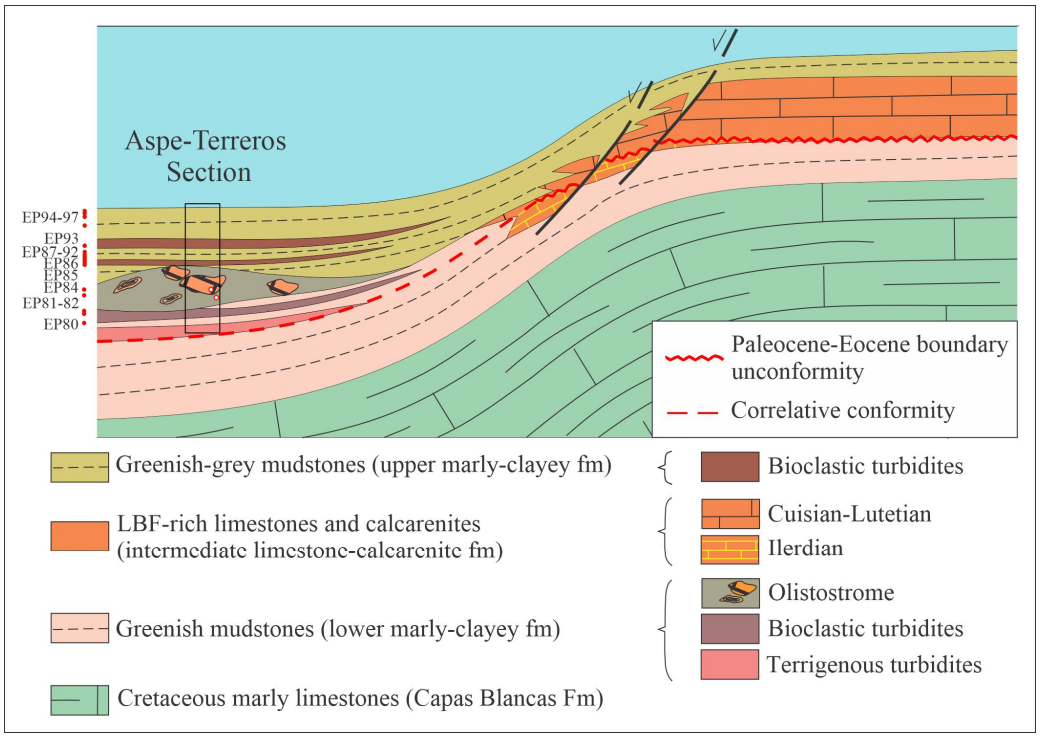


**Figure 7.** Paleogeographic section of the Eocene Prebetic platforms with the location of the Aspe-Terreros section and the hypothetic platform source of the gravity flow deposits (based on own data and [6,25–28]).

## 6. Conclusions

The Eocene Aspe-Terreros section from the Internal Prebetic in Southern Spain was studied. Three stratigraphic intervals were recognized and characterized by fine deposits on the outer ramp/upper slope platform with abundant gravity flow interlayers. The three intervals belong to the lower and upper clayey-marly fms defined in the area.

The matrix of the olistostrome and the deep-water deposits were dated using planktonic foraminifera and calcareous nannoplankton as early-middle Lutetian (E8 zone) to Bartonian (E13 and NP16–17 zones). The ages of the olistoliths and the bioclasts contained in the bioclastic turbidites were obtained using LBF (indicators of a carbonate shallow-water platform, which had been eroded) and indicate a late middle Ilerdian (SBZ8) age for the first interval, and a middle Cuisian (SBZ11) for the rest of the section.

Two main microfacies (Mf1 and Mf2) were proposed for the bioclastic turbidites and olistoliths recognized in the first and second intervals. Mf1, Ilerdian in age, indicates a source area from a mid-ramp sedimentary environment, while Mf2, Cuisian, is representative of an outer ramp/upper slope.

All the presented data, integrated with data on the region from the literature, allowed us to propose a scenario for Eocene sedimentation in the Prebetic. The background sedimentation of the area is recognized in the first and third intervals, which both indicate a muddy slope sporadically crossed by turbidity currents supplied by different sources: one terrigenous, recognized in the lowermost part of the section, the other bioclastic. The terrigenous source (derived from the Iberian Meseta) was mainly active in early Ypresian—early Lutetian.

The important novelty brought by this paper is the source that supplied the bioclasts (indicators of a carbonate shallow-water platform, which had been eroded) resedimented in the bioclastic turbidite of the first interval. It was an Ilerdian shallow water carbonate platform rich in nummulitids, which no longer exists. No carbonate platform of such age is

known in the Betic-Rif Cordilleras. The Ilerdian is part of a longer stratigraphic gap represented by the Paleocene–Eocene boundary unconformity in Betic-Rif platform domains.

The microfacies and biostratigraphic age of olistoliths are different, indicating a Cuisian platform. As such, the Ilerdian and Cuisian platforms must have been different, considering the different biostratigraphic ages and microfacies of supplied materials, and likely separated by an unconformity.

The gravity flow deposits and the above-mentioned unconformity could be the result of upper slope slumping caused by the uplifting of the source platform contemporary with the subsidence of the area where the analyzed sedimentary succession was deposited. The uplifting and subsidence may be consequences of faulting and folding related to the Paleogene tectonics (Eo-Alpine phase) together with sea-level changes. After the sedimentation of the second interval (olistostrome), the muddy sedimentation (slope) was restored. This indicates an increase in basin deepness, probably related to a tectonic quiescence.

**Supplementary Materials:** The following supporting information can be downloaded at: https://www.mdpi.com/article/10.3390/geosciences15030081/s1, Table S1: Taxonomic appendix.

**Author Contributions:** Conceptualization, J.T., M.M.-M., C.M. and J.E.T.-M.; methodology, J.T., M.M.-M., C.M., J.E.T.-M., F.S. and J.A.M.-P.; investigation, J.T., M.M.-M., C.M., J.E.T.-M., F.S. and J.A.M.-P.; data curation, J.T., M.M.-M. and C.M.; writing—original draft preparation, J.T., M.M.-M., C.M. and F.S.; writing—review and editing, J.T., M.M.-M., C.M., J.E.T.-M. and F.S.; funding acquisition, M.M.-M. All authors have read and agreed to the published version of the manuscript.

**Funding:** This research was funded by the Spanish Ministry of Science and Innovation, research project number PID2020-114381GB-I00, and the Research Projects of the Generalitat Valenciana number GVA-THINKINAZUL/2021/039.

**Data Availability Statement:** Data will be available upon request.

**Acknowledgments:** The revision performed by three anonymous reviewers is greatly acknowledged.

**Conflicts of Interest:** The authors declare no conflicts of interest.

## References

1. Martín-Martín, M.; Guerrera, F.; Tosquella, J.; Tramontana, M. Paleocene-Lower Eocene carbonate platforms of westernmost Tethys. *Sediment. Geol.* **2020**, *404*, 105674. [CrossRef]
2. Martín-Martín, M.; Guerrera, F.; Tosquella, J.; Tramontana, M. Middle Eocene carbonate platforms of the westernmost Tethys. *Sediment. Geol.* **2021**, *415*, 105861. [CrossRef]
3. Tosquella, J.; Martín-Martín, M.; Guerrera, F.; Serrano, F.; Tramontana, M. The Eocene carbonate platform of the central-western Malaguides (Internal Betic Zone, S Spain) and its meaning for the Cenozoic paleogeography of the westermost Tethys. *Palaeogeogr. Palaeoclimatol. Palaeoecol.* **2022**, *589*, 110840. [CrossRef]
4. Martín-Martín, M.; Tosquella, J.; Guerrera, F.; Maaté, A.; Hlila, R.; Maaté, S.; Tramontana, M.; Le Breton, E. The Eocene carbonate platforms of the Ghomaride Domain (Internal Rif Zone, N Morocco): A segment of the westernmost Tethys. *Sediment. Geol.* **2023**, *452*, 106423. [CrossRef]
5. Martín-Martín, M.; Tosquella, J.; Guerrera, F.; Maaté, A.; Martín-Algarra, A. The Eocene carbonate platforms of the westernmost Tethys: A review. *Int. Geol. Rev.* **2025**, *67*, 573605. [CrossRef]
6. Martín-Martín, M.; Miclaus, C.; Tent-Manclús, J.E.; Tosquella, J.; Serrano, F.; Samsó, J.M.; Martín-Pérez, J.A. Paleocene-Eocene evolution of the Prebetics (South Iberian Margin, South Spain) and comparison with other western Tethyan margins. *Mar. Pet. Geol.* **2025**, 107300. [CrossRef]
7. Vera, J.A. *Geología de España. Sociedad Geológica de España*; Instituto Geológico y Minero de España: Madrid, Spain, 2004; 884p.
8. Vera, J.A. El Terciario de la Cordillera Bética: Estado actual de conocimientos. *Rev. Soc. Geol. Esp.* **2000**, *12*, 345–373.
9. Azéma, J. Sur l'existence d'une zone intermédiaire entre Prébétique et Subbétique dans les provinces d'Alicante et de Murcie (Espagne). *Comptes Rendus Acad. Sci.* **1966**, *260*, 4020–4023.
10. Azéma, J. Géologie des confins des provinces d'Alicante et de Murcia (Espagne). *Bull. Soc. Géol. Fr.* **1966**, *8*, 80–86. [CrossRef]
11. Azéma, J. Étude Géologique des Zones Externes des Cordillères Bétiques Aux Confins des Provinces d'Alicante et de Murcie (Espagne). Doctoral Dissertation, Université Pierre et Marie Curie, Paris, France, 1977; 396p.

12. Dabrio, C.J. Geología del Sector del Alto Segura. Ph.D. Thesis, University de Granada, Granada, Spain, 1972; 388p.
13. Jérez-Mir, L. Geología de la Zona Prebética en la Transversal Elche de la Sierra y Sectores Adyacentes (Provincias de Albacete y Murcia). Ph.D. Thesis, Universidad de Granada, Granada, Spain, 1973; 750p.
14. Álvarez-Suárez, R.M.; Dabrio, C.J. Análisis e interpretación sedimentaria de la Formación de Nablanca (Eoceno, Zona Prebética). *Estud. Geol.* **1974**, *30*, 619–629.
15. Rodríguez-Estrella, T. Síntesis geológica del Prebético de la provincia de Alicante. *Bol. Geol. Min.* **1977**, *88*, 1–32.
16. Rodríguez-Estrella, T. *Geología e Hidrogeología del Sector de Alcaraz-Liétor-Yeste (Provincia de Albacete)*; Colecciones y Memorias del Instituto Geológico y Minero de España (IGME): Madrid, Spain, 1979; Volume 278, 290p.
17. García-Hernandez, M. El Jurasico Terminal y el Cretacico Inferior en las Sierras de Cazorla y Segura (Zona Prebetica). Ph.D. Thesis, University de Granada, Granada, Spain, 1978; 344p.
18. Geel, T.; Roep, T.B.; van Hinte, J.E.; Vail, P.R. Eocene tectono-sedimentary patterns in the Alicante region (Southern Spain). In *Mesozoic and Cenozoic Sequence Stratigraphy of European Basins*; Hardenbol, J., Thierry, J., Farley, J., Jacquin, T., De Graciansky, P.-C., Vail, P.R., Eds.; SEPM Special Publication: Claremore, OK, USA, 1998; Volume 60, pp. 289–302.
19. Geel, T. Recognition of stratigraphic sequences in carbonate platform and slope deposits: Empirical models based on microfacies analysis of Palaeogene deposits in southeastern Spain. *Palaeogeogr. Palaeoclimatol. Palaeoecol.* **2000**, *155*, 211–238. [CrossRef]
20. Tent-Manclus, J.E. La Estructura y Estratigrafía de las Sierras de Crevillente, Abanilla y Algayat: Su Relación Con la Falla de Crevillente. Ph.D. Thesis, Universidad de Alicante, Alicante, Spain, 2003; 1008p. Available online: http://hdl.handle.net/10045/10414 (accessed on 15 February 2025).
21. Chacón, B.; Martín-Chivelet, J. Subdivisión litoestratigráfica de las series hemipelágicas de edad Coniaciense-Thanetiense en el Prebético oriental (SE, España). *Rev. Soc. Geol. Esp.* **2005**, *18*, 3–20.
22. Pujalte, V.; Orue Etxebarria, X.; Apellaniz, E.; Baceta, J.I.; Payros, A.; Robador, A.; Tosquella, J. La Fm Puerto de La Losa (N de Granada, E de Jaén): Una nueva unidad estratigráfica, paleogeográficamente significativa, del Paleógeno Inferior Prebético. *Geogageta* **2010**, *48*, 47–50.
23. Martín-Martín, M.; Estévez, A.; Martín-Rojas, I.; Guerrera, F.; Alcalá, F.J.; Serrano, F.; Tramontana, M. The Agost Basin (Betic Cordillera, Alicante province, Spain): A pull-apart basin involving salt tectonics. *Int. J. Earth Sci.* **2018**, *107*, 655–671. [CrossRef]
24. Martín-Martín, M.; Guerrera, F.; Alcalá, F.J.; Serrano, F.; Tramontana, M. Source areas evolution in the Neogene Agost Basin (Betic Cordillera): Implications for regional reconstructions. *Ital. J. Geosci.* **2018**, *137*, 433–445. [CrossRef]
25. Martín-Chivelet, J.; Chacón, B. Event stratigraphy of the upper Cretaceous to lower Eocene hemipelagic sequences of the Prebetic Zone (SE Spain): Record of the onset of tectonic convergence in a passive continental margin. *Sediment. Geol.* **2007**, *197*, 141–163. [CrossRef]
26. Guerrera, F.; Martín-Martín, M. Geodynamic events reconstructed in the Betic, Maghrebian, and Apennine chains (central-western Tethys). *Bull. Soc. Géol. Fr.* **2014**, *185*, 329–341. [CrossRef]
27. Guerrera, F.; Estévez, A.; López-Arcos, M.; Martín-Martín, M.; Martín-Pérez, J.A.; Serrano, F. Paleogene tectono-sedimentary evolution of the Alicante Trough (External Betic Zone, SE Spain) and its bearing on the timing of the deformation of the South-Iberian Margin. *Geodin. Acta* **2006**, *19*, 87–101. [CrossRef]
28. Guerrera, F.; Mancheño, M.A.; Martín-Martín, M.; Raffaelli, G.; Rodríguez-Estrella, T.; Serrano, F. Paleogene evolution of the external betic zone and geodynamic implications. *Geol. Acta* **2014**, *12*, 171–192. [CrossRef]
29. Olsson, R.K.; Berggren, W.A.; Hemleben, C.; Huber, B.T. Atlas Paleocene Planktonic Foraminifera. In *Smithsonian Contributions to Paleobiology*; Smithsonian Institution Press: Washington, DC, USA, 1999; Volume 85, p. 252. [CrossRef]
30. Pearson, P.N.; Olsson, R.K.; Huber, B.T.; Hemleben, C.; Berggren, W.A. *Atlas of Eocene Planktonic Foraminifera*; Cushman Foundation for Foraminiferal Research, Special Publication: Glen Allen, VA, USA, 2006; Volume 41, 514p, ISBN 9781970168365.
31. Wade, B.S.; Pearson, P.N.; Berggren, W.A.; Pälike, H. Review and revision of Cenozoic tropical planktonic foraminiferal biostratigraphy and calibration to the geomagnetic polarity and astronomical time scale. *Earth-Sci. Rev.* **2011**, *104*, 11–142. [CrossRef]
32. Serra-Kiel, J.; Hottinger, L.; Caus, E.; Drobne, K.; Ferràndez, C.; Jauhri, A.K.; Less, G.; Pavlovec, R.; Pignatti, J.; Samsó, J.M.; et al. Larger foraminiferal biostratigraphy of the Tethyan Paleocene and Eocene. *Bull. Soc. Géol. Fr.* **1998**, *169*, 281–299.
33. Martini, E. Standard Tertiary and Quaternary calcareous nannoplankton zonation. In *Proceedings of the 2nd Planktonic Conference, Rome 1970*; Farinacci, A., Ed.; Tecnoscienza: Milano, Italy, 1971; pp. 739–785.
34. Flügel, E. Microfacies of carbonate rocks. In *Analysis, Interpretation and Application*; Springer: Berlin/Heidelberg, Germany, 2010; 976p.
35. Loeblich, A.R.; Tappan, H.P. *Foraminiferal Genera and Their Classification*; Van Nostrand Reinhold Company: Amsterdam, The Netherlands, 1987; Volume 2, 970p.
36. Tosquella, J.; Serra-Kiel, J. Los nummulítidos (Nummulites y Assilina) del Paleoceno Superior-Eoceno Inferior de la Cuenca Pirenaica: Sistemática. *Acta Geol. Hisp.* **1998**, *31*, 37–159.

37. Hottinger, L. Foraminifères operculiniformes: Mémoires du Museum National d'Histoire Naturelle, Serie C. *Sci. Terre* **1977**, *40*, 159.
38. Schaub, H. Nummulites et Assilines de la Tethys Paléogène: Taxinomie, phylogénèse et biostratigraphie. In *Mémoires Suisses De Paléontologie*; Birkhäuser: Basel, Switzerland, 1981; 236p.
39. Hottinger, L. Shallow benthic foraminiferal assemblages as signals for depth of their deposition and their limitations. *Bull. Soc. Géol. Fr.* **1997**, *168*, 491–505.
40. Baceta, J.I.; Mateu-Vicens, G. Seagrass development in terrigenous-influenced inner ramp settings during the middle Eocene (Urbasa–Andia Plateau, Western Pyrenees, North Spain). *Sedimentology* **2022**, *69*, 301–344. [CrossRef]
41. Mariani, L.; Coletti, G.; Bosio, G.; Vicens, G.M.; Ali, M.; Cavallo, A.; Mittempergher, S.; Malinverno, E. Tectonically-controlled biofacies distribution in the Eocene Foraminiferal Limestone (Pag, Croatia): A quantitative-based palaeontological analysis. *Sediment. Geol.* **2024**, *472*, 106743. [CrossRef]
42. Hallock, P.; Glenn, E.C. Larger foraminifera: A tool for paleoenvironmental analysis of Cenozoic carbonate depositional facies. *Palaios* **1986**, *1*, 55–64. [CrossRef]
43. Buxton, M.W.N.; Pedley, H.M. Short Paper: A standardized model for Tethyan Tertiary carbonate ramps. *J. Geol. Soc. Lond.* **1989**, *146*, 746–748. [CrossRef]
44. Burchette, T.P.; Wright, V.P. Carbonate ramp depositional systems. *Sediment. Geol.* **1992**, *79*, 3–57. [CrossRef]
45. Gebhardt, H.; Coric, S.; Darga, R.; Briguglio, A.; Schenk, B.; Werner, W.; Andersen, N.; Sames, B. Middle to late Eocene paleoenvironmental changes in a marine transgressive sequence from the northern Tethyan margin (Adelholzen, Germany). *Austrian J. Earth Sci.* **2013**, *106*, 45–72. [PubMed]
46. Mateu-Vicens, G.; Pomar, L.; Ferrandez-Canadell, C. Nummulitic banks in the upper Lutetian 'Buil level', Ainsa Basin, South Central Pyrenean Zone: The impact of internal waves. *Sedimentology* **2012**, *59*, 527–552. [CrossRef]
47. Pomar, L.; Baceta, J.I.; Hallock, P.; Mateu-Vicens, G.; Basso, D. Reef building and carbonate production modes in the west-central Tethys during the Cenozoic. *Mar. Pet. Geol.* **2017**, *83*, 261–304. [CrossRef]
48. Hlila, R.; Maaté, A.; Sanz de Galdeano, C.; Serra-Kiel, J.; Serrano, F.; El Kadiri, K. La serie paleógena de la unidad superior del Gomáride en Talembote (Rif Interno, Marruecos). *Geogaceta* **2007**, *43*, 91–94.
49. Bosence, D. A genetic classification of carbonate platforms based on their basinal and tectonic settings in the Cenozoic. *Sediment. Geol.* **2005**, *175*, 49–72. [CrossRef]
50. Guerrera, F.; Martín-Martín, M.; Tramontana, M. Evolutionary geological models of the central-western peri-Mediterranean chains: A review. *Int. Geol. Rev.* **2021**, *63*, 65–86. [CrossRef]